Evaluation of spontaneous propulsive movement as a screening tool to detect phenotypic rescue in zebrafish models of Parkinsonism

Thomas C. Farrell, Clinton L. Cario, Chiara Milanese, Andreas Vogt, Jong-Hyeon Jeong and Edward A. Burton

Supplementary Data

Supplementary Figure 1 – Methodology for measuring zebrafish larval movement in multiwell plates

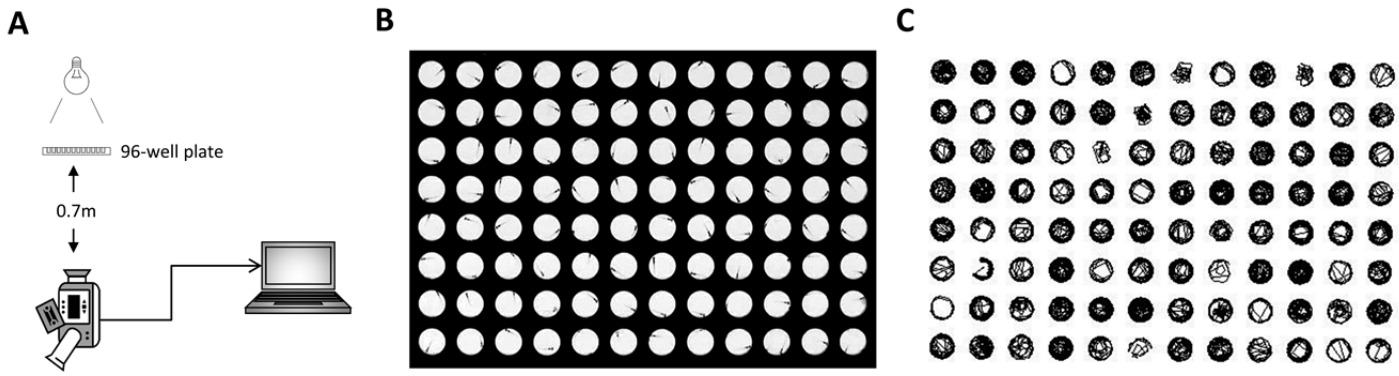

A: Zebrafish were housed in E3 buffer within multiwell plates inside an incubator to control temperature and remove extraneous stimuli. The plate was illuminated from above and the video camera positioned beneath the plate in order to avoid optical artifacts relating to the surface meniscus. The plate was housed within a chamber containing an open reservoir of E3 to minimize evaporation during prolonged recordings.

B: Video was captured by streaming directly to a computer; the image shows a single video frame of a 96-well plate where each trans-illuminated well contains a single zebrafish larva at 7dpf.

C: Video recordings were analyzed using custom Matlab applications, which identified each larva in each frame of the video and then calculated vector displacement of its centroid from the previous frame. The image shows the loci traversed by each larva in a 96-well plate over a 10-minute recording period, to illustrate the tracking analysis. V_M for each larva was calculated as its total displacement over the course of a recording divided by the time of the recording. T% for each larva was calculated as the proportion of video frames in which the larva showed displacement above noise levels from the previous frame. V_A was calculated as the total displacement of each larva divided by the time occupied by frames where displacement from the previous frame was above noise levels.

Supplementary Figure 2 - Optimization of recording parameters

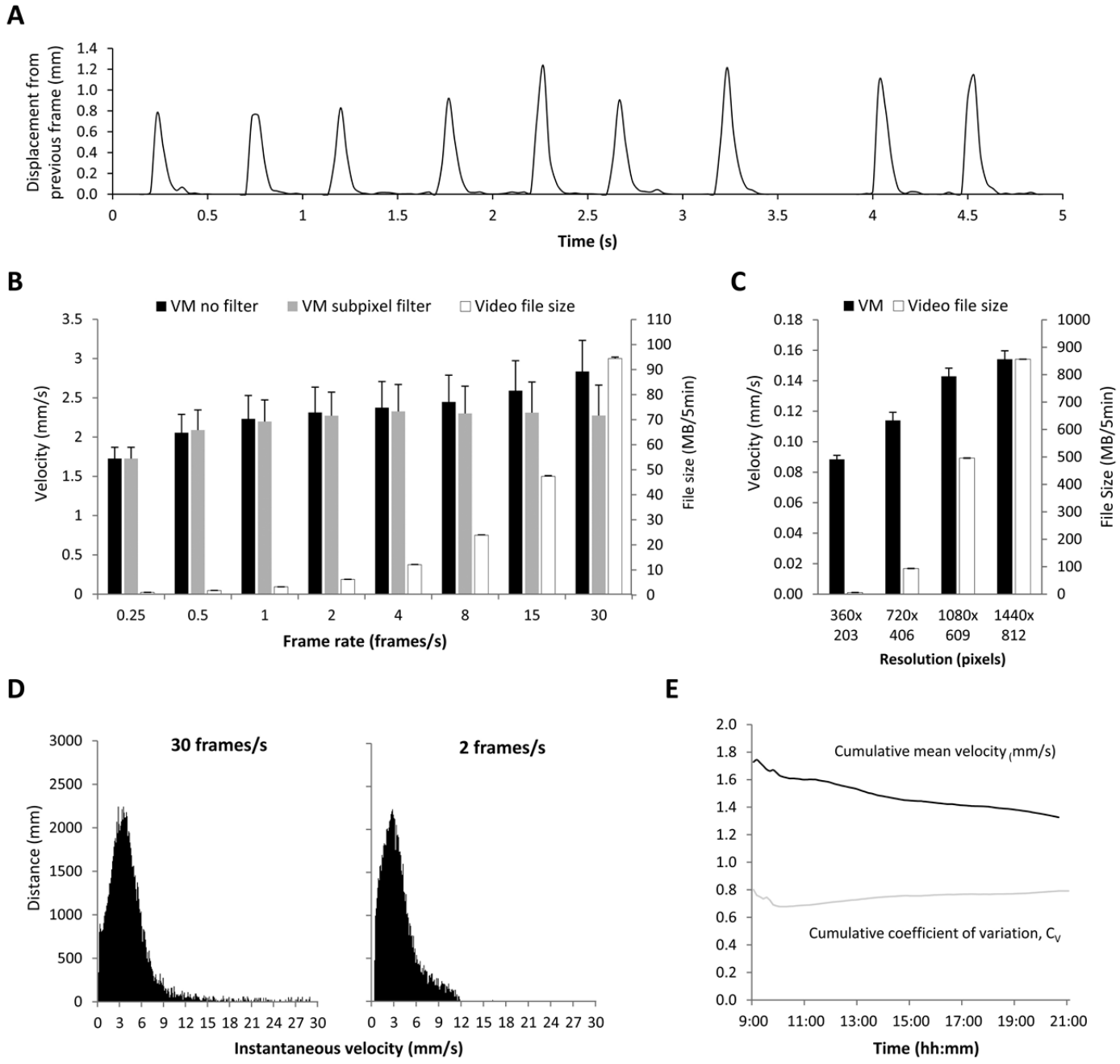

A: Recordings carried out at 30 frames/s and 1440 x 812 pixels enabled characterization of the types of spontaneous movements that larval zebrafish produce in multiwell plates. Most of the movements fell into two categories – small rotational movements, in which larvae change their orientation with respect to the edge of the well, and larger propulsive movements in which larvae move around the edge of the well (or across the well in 24-well plates or plates with larger wells). Propulsive movements, as shown in this instantaneous velocity/time graph, accounted for most of the total displacement that occurred during a recording period and showed a mean duration of approximately 200ms, with a minimum interval between the onset of successive movements of ≈500ms (see video).

B: We examined how video frame rate affected the measurement of movement. A single 30 frames/s DV tape recording was captured digitally at different frame rates, and the amount of movement, expressed as V_M, calculated after tracking.

Stochastic pixel noise causes small sub-pixel displacements of the larval centroid from frame to frame – this is not associated with visible larval movement and can occur at any frame transition – consequently spurious movement attributable to noise increases proportionately to the number of frames. This can be filtered by removing sub-pixel displacements prior to analysis. However, larval movements start to overlap in amplitude with pixel noise at high frame rates, and a sub-pixel filter in this case removes some of the movement in addition to noise. Above 4 frames/s the true displacement is somewhere between the values shown with and without the filter. Interestingly, for recording overall displacement, there is little advantage in using a frame rate above 2 frames/s. At 2 frames/s, ≈90% of the displacement recorded at 30 frames/s is captured, while the video file size is <10% that generated at 30 frames/s. In addition, analysis takes ≈$1/15^{th}$ of the time taken to analyze a 30 frames/s recording of the same duration. Consequently, we carried out all of the experiments in this report at 2 frames/s; in addition to allowing live video streaming, this low frame rate obviated the need to apply a noise filter.

C: At a frame rate of 2 frames/s, the measured displacement increased approximately linearly with increasing resolution, whereas video file size increased exponentially. A resolution of 720x406 pixels captured >80% of the movement recorded at 1440x812 pixels, whereas the resulting video file size was only 12% of the size, and video could be streamed live via a IEEE1394 connection.

D: T% and V_A are calculated by assigning frames as either showing displacement or no displacement from the previous frame; consequently, they vary according to the criteria used to determine whether a movement has occurred. After filtering subpixel noise as described above, T% was not significantly different between analysis at different frame rates (51.4% ± 5.3% at 30 frames/s versus 48.6% ± 6.2% at 30 frames/s, p=0.19, paired T-test), whereas V_A was higher at the faster frame rate (2.77 ± 0.17 mm/s at 30 frames/s versus 2.34 ± 0.11 mm/s at 2 frames/s, p= 0.00075, paired T-test). The distributions of instantaneous velocities measured at the different frame rates were similar as illustrated in these histograms showing the amount of displacement that was recorded at each instantaneous velocity during a recording. However, uncommon high velocity movements recorded at 30 frames/s were compressed into lower velocity bins at 2 frames/s as a result of the longer time base between data points. V_A and T% can be estimated from recordings at 2 frames/s, although movement duration and peak velocity would require higher frame rates.

E: Over the course of a day, larvae showed gradually declining mobility. The coefficient of variation for V_M had stabilized by 3 – 4 hours into the recording, suggesting that this was the minimal recording period that would give an accurate measure of movement and its variability. A separate power analysis of a large sample with known mean and variation suggested a minimum recording time of 2hr 50 min was required. All of the data reported here were obtained from 3 – 4 hour recordings starting at 9AM.

Supplementary Figure 3 – Relative sizes of larvae and wells

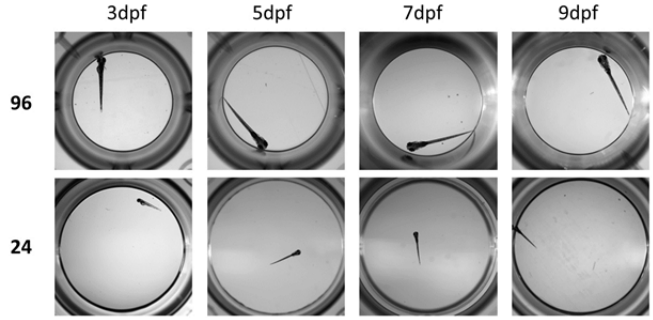

The photographs show the sizes of larvae of different ages (3, 5, 7, 9dpf indicated above the images) relative to the wells of 96 or 24-well plates.

Supplementary Figure 4 – Concentration-response curves for dopaminergic agents

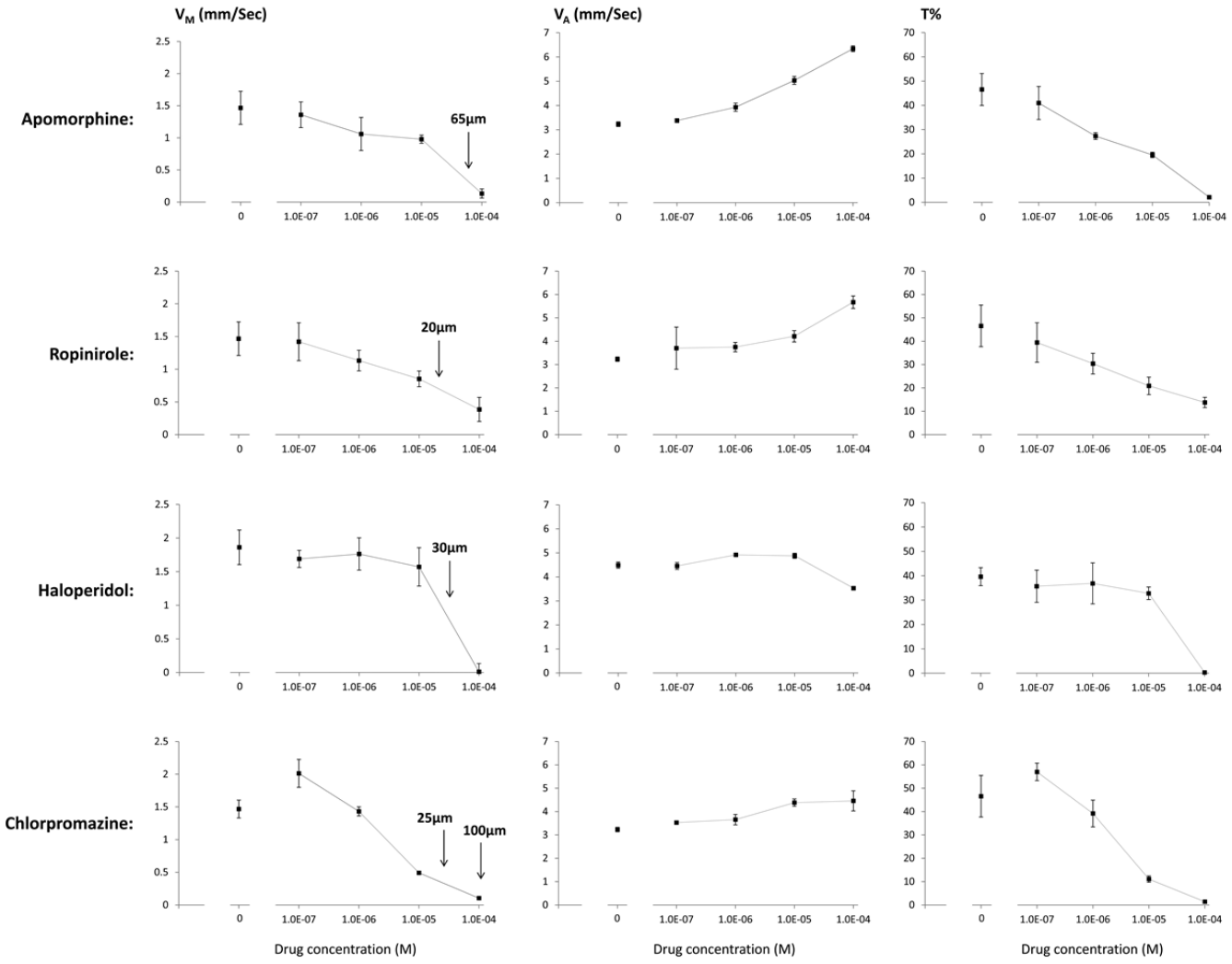

The graphs show example concentration-response curves for the dopaminergic agents used in figures 3 and 4. A wide range of doses is depicted logarithmically on the X-axis, and the measured values for V_M, V_A and T% shown on the Y-axes. Each data point shows the mean of 8 larvae, error bars show standard error of mean. These data were used to find concentration ranges in which the trends shown in the graphs were clearly demonstrated for subsequent experiments, such as the bar charts shown in figures 3A and C and the assay characterizations shown in figure 4; the concentrations used for these subsequent experiments are indicated above the V_M dose-response curves for each drug.

Supplementary Video 1 – Comparison of frame rates to capture larval movement

The video shows a comparison of the same video recording at 30 frames/s (right panel) and 2 frames/s (left panel) to illustrate the analysis described in figure S2, both pictorially and intuitively: the lower frame rate captures most of the displacement but loses details and temporal resolution of the movements. Since we were primarily interested in developing a screening tool that could deploy low bandwidth information to allow high-throughput assays using simple equipment, we carried out all experiments in this study at 2 frames/s and limited our analysis to displacement, active velocity and proportion of time moving.